

$B_s \rightarrow \mu^+ \mu^-$ and $\bar{B} \rightarrow X_s \gamma$ to NNLO

Matthias Steinhauser^{*†}

Institut für Theoretische Teilchenphysik, Karlsruhe Institute of Technology (KIT),

D-76128 Karlsruhe, Germany

E-mail: matthias.steinhauser@kit.edu

In this contribution, the recent calculation of next-to-next-to-leading order QCD and next-to-leading order electroweak corrections to the decay $B_s \rightarrow \mu^+ \mu^-$ is reviewed, and a detailed discussion of the uncertainty of the theory prediction is provided. Furthermore, we discuss the status of the next-to-next-to-leading order QCD corrections to $\bar{B} \rightarrow X_s \gamma$.

Loops and Legs in Quantum Field Theory - LL 2014,

27 April - 2 May 2014

Weimar, Germany

^{*}Speaker.

[†]This work was supported by the DFG through the SFB/TR 9 “Computational Particle Physics”. I would like to thank Christoph Bobeth, Martin Gorbahn, Thomas Hermann, Mikołaj Misiak, and Emmanuel Stamou for a fruitful collaboration on the subject of this contribution.

1. Introduction

In the last decades, the Standard Model (SM) of particle physics has been confirmed at many different energy scales, and there are only a few processes where deviations at the level of $2 - 3\sigma$ are observed. Nevertheless, there are several questions where the SM cannot provide a satisfactory answer, which triggers a huge activity — both on the theory and on the experimental side — to search for deviations and thus for hints of physical phenomena in accordance with extended theories. A very promising place to look for discrepancies with SM predictions are processes related to B mesons since on the one hand there are precise measurements available, and on the other hand it is possible to perform precision calculations, and to arrive at rigorous predictions. Among the most promising processes there are the decays of a B_s meson into two muons, and of a B meson into a meson containing a strange quark and a photon. It is common to both of them that the SM contribution is loop-induced, and thus potential new physics effects are parametrically of the same order of magnitude, which can hence lead to sizable effects. Whereas the branching ratio in the case of $\bar{B} \rightarrow X_s \gamma$ is of the order 10^{-4} , it is of the order 10^{-9} for $B_s \rightarrow \mu^+ \mu^-$.

The main part of this proceedings contribution deals with $B_s \rightarrow \mu^+ \mu^-$. End of 2013 next-to-next-to-leading order (NNLO) QCD and NLO electroweak (EW) corrections became available [1, 2, 3] which we briefly review in Section 2. Afterwards, in Section 3, the theory prediction is discussed where special emphasis is put on the corresponding uncertainty.

NNLO corrections to $\bar{B} \rightarrow X_s \gamma$ have been computed in Refs. [4, 5]. In Section 4 we provide a brief status of the updated prediction for the branching ratio based on improved theoretical input.

2. NNLO QCD and NLO EW corrections to $B_s \rightarrow \mu^+ \mu^-$

There are several energy scales involved in decays of B mesons: first of all there is the typical scale of the decay process, μ_b , which is of the order of the bottom quark mass. Furthermore, there are masses of the virtual particles in the loops, which in the SM are essentially given by the W boson and the top quark. In the following, the latter scale is denoted by μ_0 . The framework which can be used to perform calculations involving widely separated scales is based on an effective theory where the heavy degrees of freedom are integrated out from the underlying theory. In the case at hand, this leads to an effective Lagrange density with only one relevant effective operator¹ $Q_A = (\bar{b}\gamma_\alpha\gamma_5 s)(\bar{\mu}\gamma^\alpha\gamma_5\mu)$. In order to arrive at predictions for the decay rate, the corresponding matching coefficient, C_A , has to be computed in a first step at the high scale μ_0 . Afterwards, it has to be evolved to μ_b using renormalization group techniques.

The one-loop calculation of C_A has been performed for the first time in Ref. [6], and NLO QCD corrections have been considered in Refs. [7, 8, 9, 10]. Recently, the three-loop corrections, $C_A^{(2)}$, have been computed in Ref. [1]. The calculation can be reduced to vacuum integrals involving the two masses M_W and m_t , which have been solved with the help of expansions for $m_t \gg M_W$ and $m_t \approx M_W$. In this way, only one-scale integrals have to be computed and simple analytic results are obtained, which are of polynomial form with at most logarithmic coefficients. Thus, the numerical evaluation is simple and straightforward.

¹In beyond-SM theories sizable contributions are also obtained from operators with scalar and pseudo-scalar currents.

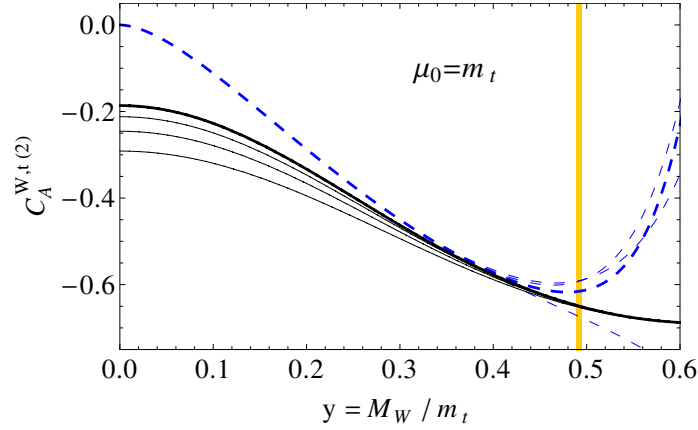


Figure 1: Three-loop corrections to the W -box contribution to $C_A^{(2)}$ involving W -top-bottom vertices. Solid lines result from expansions around $y = 1$ and dashed lines are obtained for $y \ll 1$.

As an exemplary case we show in Fig. 1 the result for the W -box contribution to $C_A^{(2)}$ from diagrams with W -top-bottom vertices as a function of $y = M_W/m_t$. The solid (black) lines originate from the expansion around $y = 1$, and the dashed (blue) lines from the case $y \ll 1$. Thinner lines correspond to results involving less expansion terms. One observes that deviations only occur either below or above $y \approx 0.4$, which leads to the conclusion that the combination of the expansions provide an excellent approximation to $C_A^{(2)}$ in the whole range $y \in [0, 1]$. In particular, in the physical region for y , which is indicated by the vertical (yellow) band, the expansion around the equal-mass limit alone is sufficient to provide a three-loop prediction. The inclusion of the three-loop QCD corrections to C_A reduces the uncertainties to the branching ratio from scale variation of μ_0 in the interval $m_t/2$ to $2m_t$ from 1.8% to below 0.2% [1].

The complete NLO EW corrections have been computed in Ref. [2]. Before, only the leading m_t^2 terms were known from Ref. [11] and the corresponding uncertainties have been estimated to be of the order of about 7%. In contrast to QCD, there is a non-trivial running of C_A from μ_0 to μ_b after including $\mathcal{O}(\alpha_{em})$ terms which originate from mixing of operators once QED corrections are turned on [12, 13, 14]. In Ref. [2] this effect has been taken into account together with a detailed study of the renormalization scheme dependence. The results are shown in Fig. 2 where $\tilde{c}_{10} = -2C_A$ is plotted for four different choices (see Ref. [2] for details) at LO and NLO. One observes huge differences at LO (dotted line) which basically disappear at NLO (solid line).

3. Prediction for $\overline{\mathcal{B}}(B_s \rightarrow \mu^+ \mu^-)$

In 2013 the CMS and LHCb experiments at the LHC have provided measurements for the averaged time-integrated branching ratios for $B_s \rightarrow \mu^+ \mu^-$ and $B_d \rightarrow \mu^+ \mu^-$. The combination [15] given by

$$\overline{\mathcal{B}}_{s\mu} = (2.9 \pm 0.7) \times 10^{-9}, \quad \overline{\mathcal{B}}_{d\mu} = (3.6_{-1.4}^{+1.6}) \times 10^{-10}, \quad (3.1)$$

is based on the measurements [16] and [17]. In the forthcoming decade a reduction of the uncertainties to a few percent level is expected, in particular for $\overline{\mathcal{B}}_{s\mu}$, in which case the uncertainty

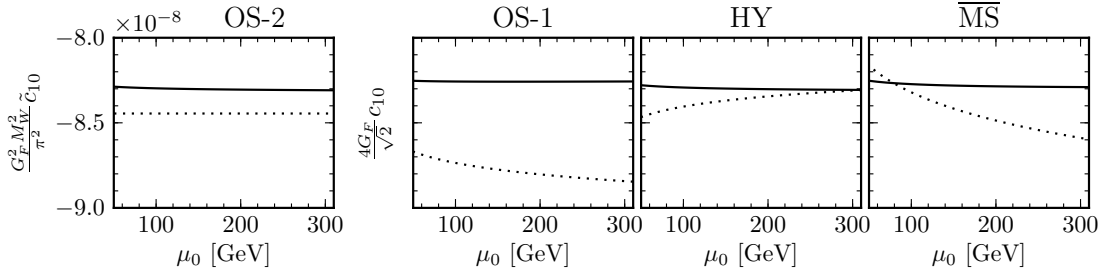


Figure 2: NLO electroweak corrections adopting different renormalization schemes.

is to a large extent dominated by statistics. In Ref. [3] the numbers in Eq. (3.1) have been confronted with theory predictions including NNLO QCD and NLO EW corrections, as discussed in Section 2. In the following, we concentrate on $B_s \rightarrow \mu^+ \mu^-$; the arguments hold analogously also for $B_d \rightarrow \mu^+ \mu^-$.

Within the effective-theory framework the branching ratio $\bar{\mathcal{B}}_{s\mu}$ can be cast in the form (see also Ref. [18])

$$\bar{\mathcal{B}}_{s\mu} = \frac{|N|^2 M_{B_s}^3 f_{B_s}^2}{8\pi \Gamma_H^s} \beta_{s\mu} r_{s\mu}^2 |C_A(\mu_b)|^2 + \mathcal{O}(\alpha_{em}), \quad (3.2)$$

with $N = V_{tb}^* V_{ts}$, $G_F^2 M_W^2 / \pi^2$, $r_{s\mu} = 2m_\mu / M_{B_s}$, $\beta_{s\mu} = \sqrt{1 - r_{s\mu}^2}$ and Γ_H^s denoting the heavier mass-eigenstate total width. M_{B_s} is the B_s -meson mass, and f_{B_s} its decay constant which is defined by the QCD matrix element $\langle 0 | \bar{b} \gamma^\alpha \gamma_5 s | B_s(p) \rangle = i p^\alpha f_{B_s}$. The term “ $\mathcal{O}(\alpha_{em})$ ” originates from the fact that NLO QED corrections to $\bar{\mathcal{B}}_{s\mu}$ are not complete as virtual NLO corrections to the matrix element $\langle \mu^+ \mu^- | Q_A | B_s \rangle$ are missing. It has been estimated to be of the order of 0.3%, which is based on the following observations:

- The $\mathcal{O}(\alpha_{em})$ term in Eq. (3.2) does not contain any enhancement factor like m_t^2 / M_W^2 or $1 / \sin^2 \Theta_W$. Such factors are present in the genuine NLO EW corrections of Ref. [2].
- Soft photon bremsstrahlung can potentially lead to sizeable $\mathcal{O}(\alpha_{em})$ corrections. The dimuon invariant-mass spectrum for the decay rate $B_s \rightarrow \mu^+ \mu^- (n\gamma)$ with $n = 0, 1, 2, \dots$ is shown in Fig. 3 where the (blue) dotted curve corresponds to real photon emission from the quarks, which has been discussed in Ref. [19]. The red curve is supposed to contain all other $\mathcal{O}(\alpha_{em})$ corrections, in particular the soft photon radiation from the muons [20] which constitutes the dominant part.

As can be seen, the (blue) dotted curve is highly suppressed in the signal regions of CMS and LHCb which are indicated by the dashed and dash-dotted vertical lines. This contribution is infrared safe because the decaying meson is electrically neutral. On the experimental side it is (should be) treated as background and it is not considered at all in the theory prediction.

On the other hand, the photon bremsstrahlung from the muons is taken into account in both experimental analyses with the help of the program PHOTOS [21] which is used to extrapolate along the solid (red) curve down to zero. Thus, in the resulting quantity there are

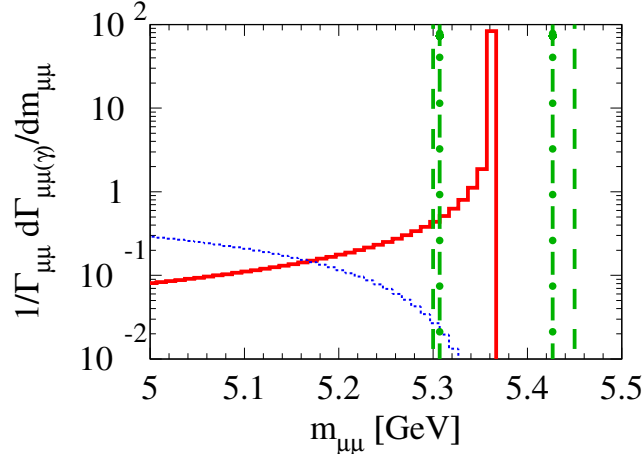


Figure 3: Contributions to the dimuon invariant-mass spectrum in $B_s \rightarrow \mu^+ \mu^- (n\gamma)$ with $n = 0, 1, 2, \dots$. The (blue) dotted curve describes the contribution from photons radiated off a quark line, whereas the (red) solid line originates from photonic corrections to the muon line. Both of them are displayed in bins of 0.01 GeV width. The (green) vertical lines indicate the blinded signal windows of the CMS (dashed) and LHCb (dash-dotted) experiments.

no large QED logarithms, which in principle could emerge from the applied cuts, and one remains with a usual $\mathcal{O}(\alpha_{em})$ correction without extra enhancement.

- One has to worry about the question whether it is possible that QED corrections of order $\alpha_{em}/\pi \approx 2 \times 10^{-3}$ can remove a helicity suppression factor $m_\mu^2/M_{B_s}^2 \approx 10^{-4}$ and thus lead to correction terms which have to be taken into account. The following reasons show that this is not the case
 - Virtual $\mathcal{O}(\alpha_{em})$ corrections both on the quark and muon line cannot undo the helicity suppression in the SM since then the same argument holds as at LO and the vector or axial-vector lepton currents will always lead to suppression factors $m_\mu^2/M_{B_s}^2$ in the branching ratio.
 - Real photon corrections of order α_{em} off a muon still lead to helicity suppression because the QCD matrix element defining f_{B_s} is proportional to p^α which is the momentum flowing into the vector or axial-vector lepton current. Since the latter is conserved for massless leptons, helicity suppression remains in action.
 - Real photon corrections from the quarks can lift the helicity suppression, however, the corresponding contribution is highly phase space suppressed in the signal region [19], as is shown by the blue line in Fig. 3.
 - Real photon corrections from the muon can lift the helicity suppression only in case there is a further virtual photon connecting the quark and muon line. In that case the above argument is not valid, however, we have a suppression factor α_{em}^3 for the branching ratio, which is significantly smaller than $m_\mu^2/M_{B_s}^2$.

		f_{B_q}	CKM	τ_H^q	M_t	α_s	other param.	non-param.	Σ
$\overline{\mathcal{B}}_{s\mu}$	$(3.65 \pm 0.23) \times 10^{-9}$	4.0%	4.3%	1.3%	1.6%	0.1%	< 0.1%	1.5%	6.4%
$\overline{\mathcal{B}}_{d\mu}$	$(1.06 \pm 0.09) \times 10^{-10}$	4.5%	6.9%	0.5%	1.6%	0.1%	< 0.1%	1.5%	8.5%

Table 1: Central value and relative uncertainties from various sources for $\overline{\mathcal{B}}_{s\mu}$ and $\overline{\mathcal{B}}_{d\mu}$. In the last column they are added in quadrature.

- The $\mathcal{O}(\alpha_{em})$ has to cancel the μ_b dependence of $|C_A(\mu_b)|^2$ which amounts to 0.3% when varying μ_b between $m_b/2$ and $2m_b$.

At that point it is straightforward to evaluate the branching ratio. We refrain from repeating the discussion about the input parameters which can be found in Ref. [3] but want to mention a few important issues in connection to the uncertainty of the branching ratio. A summary is given in Table 1.

- The largest contributions to the uncertainties arise from the decay constants and the CKM matrix elements. The former is based on lattice determinations, and the values for f_{B_s} and f_{B_d} are taken over from a compilation of the Flavour Lattice Averaging Group (FLAG) [22].
- In the case of B_s , we write the CKM factors $|V_{tb}^* V_{ts}|$ as $|V_{cb}| \times |V_{tb}^* V_{ts}/V_{cb}|$, which allows us to use numerical results for the accurately known ratio $|V_{tb}^* V_{ts}/V_{cb}|$. Furthermore, a precise result for $|V_{cb}|$ has recently been obtained in Ref. [23] taking into account both the semileptonic data and the precise quark mass determinations from flavor-conserving processes.
- The parameters M_t (on-shell top quark mass) and α_s enter the matching coefficient $C_A(\mu_b)$ in a non-trivial way. In Ref. [3] formulae for the branching ratio are provided which allow for a convenient change of these parameters.
- The column “other param.” in Table 1 shows that the uncertainties originating from the not explicitly listed parameters (like the Higgs or gauge boson masses or the Fermi constant) are negligible.
- The contributions to the non-parametric uncertainties, which are estimated to 1.5% both for $\overline{\mathcal{B}}_{s\mu}$ and $\overline{\mathcal{B}}_{d\mu}$ include

$\mathcal{O}(\alpha_{em})$ in Eq. (3.2)	0.3%
NNLO QCD μ_0 dependence	0.2%
NLO EW μ_0 dependence	0.2%
NLO EW renormalization scheme dependence	0.6%
Higher-order $M_{B_q}^2/M_W^2$ power corrections	0.4%
$\overline{\text{MS}}$ –OS top quark mass conversion	0.3%

Combining these uncertainties in quadrature would give 0.9%. Our overall estimate of 1.5% is somewhat more conservative.

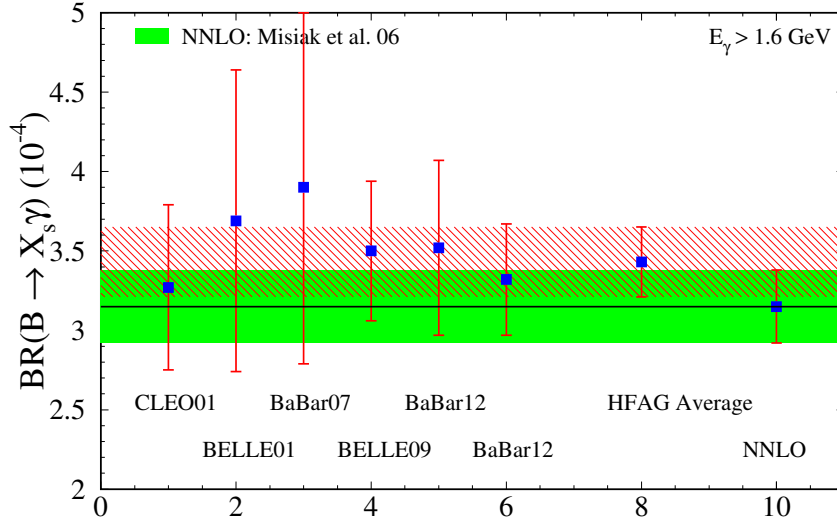


Figure 4: Compilation of experimental results for $\bar{B} \rightarrow X_s \gamma$ with a cut on the photon of $E_\gamma > 1.6$ GeV, and comparison to SM theory prediction from Ref. [4, 5].

- In total relative uncertainties of 6.4% and 8.5% are obtained for $\bar{\mathcal{B}}_{s\mu}$ and $\bar{\mathcal{B}}_{d\mu}$, respectively.

4. $\bar{B} \rightarrow X_s \gamma$

There are a number of experiments which have measured the branching ratio $\bar{\mathcal{B}}(\bar{B} \rightarrow X_s \gamma)$ with high accuracy. A compilation of results from CLEO [24], BaBar [25, 26, 27] and BELLE [28, 29] is shown in Fig. 4 where the hatched (red) uncertainty band corresponds to a combination performed by the Heavy Flavour Averaging Group (HFAG) [30]. The experimental result is compared to the theory prediction of Refs. [4, 5] (solid, green band). One observes a significant overlap of the two bands which indicates a good agreement of the experimental number with the SM prediction. Both uncertainty bands amount to approximately 7%. Once Belle II starts data taking it is expected that the experimental uncertainty will shrink, which calls for an improvement on the theory side.

The theory uncertainty band in Fig. 4 receives contributions from unknown higher order (3%), input parameters (3%), “ m_c -interpolation” (3%), and non-perturbative effects (5%). Near-future improvements can be expected from improved measurements of the input parameters and new calculations of the charm-quark contributions to the four-quark operators Q_1 and Q_2 , which might improve the “ m_c -interpolation” uncertainty. An analysis containing an improved prediction is in preparation [31].

References

- [1] T. Hermann, M. Misiak and M. Steinhauser, JHEP **1312**, 097 (2013) [arXiv:1311.1347].

- [2] C. Bobeth, M. Gorbahn and E. Stamou, Phys. Rev. D **89**, 034023 (2014) [arXiv:1311.1348].
- [3] C. Bobeth, M. Gorbahn, T. Hermann, M. Misiak, E. Stamou and M. Steinhauser, Phys. Rev. Lett. **112** (2014) 101801 [arXiv:1311.0903 [hep-ph]].
- [4] M. Misiak, H. M. Asatrian, K. Bieri, M. Czakon, A. Czarnecki, T. Ewerth, A. Ferroglia and P. Gambino *et al.*, Phys. Rev. Lett. **98** (2007) 022002 [hep-ph/0609232].
- [5] M. Misiak and M. Steinhauser, Nucl. Phys. B **764** (2007) 62 [hep-ph/0609241].
- [6] T. Inami and C. S. Lim, Prog. Theor. Phys. **65** (1981) 297 [Erratum-ibid. **65** (1981) 1772].
- [7] G. Buchalla and A. J. Buras, Nucl. Phys. B **398** (1993) 285.
- [8] G. Buchalla and A. J. Buras, Nucl. Phys. B **400** (1993) 225.
- [9] M. Misiak and J. Urban, Phys. Lett. B **451** (1999) 161 [hep-ph/9901278].
- [10] G. Buchalla and A. J. Buras, Nucl. Phys. B **548** (1999) 309 [hep-ph/9901288].
- [11] G. Buchalla and A. J. Buras, Phys. Rev. D **57** (1998) 216 [hep-ph/9707243].
- [12] C. Bobeth, P. Gambino, M. Gorbahn and U. Haisch, JHEP **0404**, 071 (2004) [hep-ph/0312090].
- [13] T. Huber, E. Lunghi, M. Misiak and D. Wyler, Nucl. Phys. B **740**, 105 (2006) [hep-ph/0512066].
- [14] M. Misiak, in Proceedings of 15th Lomonosov Conference on Elementary Particle Physics (Moscow, Russia, August 18-24, 2011), p. 301, [arXiv:1112.5978].
- [15] CMS and LHCb Collaborations, EPS-HEP 2013 European Physical Society Conference on High Energy Physics, Stockholm, Sweden, 2013, Conference Report No. CMS-PAS-BPH-13-007, LHCb-CONF-2013-012, <http://cds.cern.ch/record/1564324>.
- [16] S. Chatrchyan *et al.* (CMS Collaboration), Phys. Rev. Lett. **111**, 101804 (2013) [arXiv:1307.5025].
- [17] R. Aaij *et al.* (LHCb Collaboration), Phys. Rev. Lett. **111** 101805, (2013) [arXiv:1307.5024].
- [18] K. De Bruyn *et al.*, Phys. Rev. Lett. **109**, 041801 (2012) [arXiv:1204.1737].
- [19] Y. G. Aditya, K. J. Healey and A. A. Petrov, Phys. Rev. D **87**, 074028 (2013) [arXiv:1212.4166].
- [20] A. J. Buras, J. Girrbach, D. Guadagnoli and G. Isidori, Eur. Phys. J. C **72**, 2172 (2012) [arXiv:1208.0934].
- [21] P. Golonka and Z. Was, Eur. Phys. J. C **45**, 97 (2006) [hep-ph/0506026].
- [22] S. Aoki *et al.* (Flavour Lattice Averaging Group), arXiv:1310.8555; updates at <http://itpwiki.unibe.ch/flag>.
- [23] P. Gambino and C. Schwanda, Phys. Rev. D **89**, 014022 (2014) [arXiv:1307.4551].
- [24] S. Chen *et al.* [CLEO Collaboration], Phys. Rev. Lett. **87** (2001) 251807 [hep-ex/0108032].
- [25] B. Aubert *et al.* [BaBar Collaboration], Phys. Rev. D **77** (2008) 051103 [arXiv:0711.4889 [hep-ex]].
- [26] J. P. Lees *et al.* [BaBar Collaboration], Phys. Rev. D **86** (2012) 052012 [arXiv:1207.2520 [hep-ex]].
- [27] J. P. Lees *et al.* [BaBar Collaboration], Phys. Rev. Lett. **109** (2012) 191801 [arXiv:1207.2690 [hep-ex]].
- [28] K. Abe *et al.* [Belle Collaboration], Phys. Lett. B **511** (2001) 151 [hep-ex/0103042].
- [29] A. Limosani *et al.* [Belle Collaboration], Phys. Rev. Lett. **103** (2009) 241801 [arXiv:0907.1384 [hep-ex]].
- [30] Heavy Flavour Averaging Group (HFAG), <http://www.slac.stanford.edu/xorg/hfag/>
- [31] M. Czakon, P. Fiedler, T. Huber, M. Misiak, T. Schutzmeier and M. Steinhauser, in preparation.